Journal of Computers Vol. 28, No. 4, 2017, pp. 49-62
doi:10.3966/199115592017082804006

# Analysis of Handover Decision with Adaptive Offset and Link Quality Threshold in Next-Generation Hybrid Macro/Femto-cell Networks

Min-Shu Hung[1], Jen-Yi Pan[1*], and Yu-Chen Hsieh[1]

[1] Department of Communications Engineering,
National Chung Cheng University
Chia-Yi 621, Taiwan, ROC
jypan@comm.ccu.edu.tw

Received 6 July 2015; Revised 27 December 2016; Accepted 27 December 2016

Abstract. Femto base stations are usually installed in the region of macrocells in next-generation hybrid macro/femto-cell networks, and the transmit power of macro base stations is much larger than that of femto base stations. Because the conventional handover decision is only based on the received signal strength (RSS), user equipments near the center of macrocells hardly camp on femtocells, even if the RSS of femtocells satisfies the link quality requirement. In order to offload more users from macro to femto base stations, a cell-specific virtual offset is added to the RSS to artificially expand the cell range of the femto base stations. We analyze handover decision performance with adaptive offset. When the RSS of femtocells satisfies the link quality threshold, the algorithm compensates large differences between RSS measurements of macrocells and femtocells by a priori setting a femtocell boundary, indicating user equipments to stay inside the expected coverage of femtocells. We mathematically assess the algorithm in a log-distance path loss and log-normal shadowing environment, and compare it with the conventional one under two different trajectories, moving forward and perpendicular. The numerical results show that with our adapted offset the algorithm can efficiently raise the utility of femtocells and reduce unnecessary handover numbers.

Keywords: cell range expansion (CRE), femto BS, handover, heterogeneous network (HetNet), long term evolution (LTE)

## 1 Introduction

A mobile access network with hierarchical cell structures is covered by a number of cells with different coverage and capacity, each served by a base station with different transmit power and bandwidth, configured by operators according to their deployment plan. These cells are classified as macrocell, microcell, femtocell, and femtocell according to coverage size. They can provide high service quality for indoor mobile users, and even sometimes can also provide services to outdoor users. In a hierarchical cell structure mentioned above, a large number of low-power femto base stations (BSs) are deployed in the coverage area of macro BSs. However, typical values of transmit power of femto BSs and macro BSs are about 20 dBm and 46 dBm, respectively [1]. When the femto BS is installed in the center or inner region of the macrocell, the measured RSS of macro BSs is often greater than the measured RSS of femto BSs, resulting in that the handover criterion from a macrocell to a femtocell is hardly satisfied, even though the path loss to the femtocell is lower and the link quality of the femtocell is fairly well. In order to improve utilization of femto BSs, a virtual offset can be added to the measured RSS of femto BSs [6-7], called cell range expansion. To our best knowledge, properly setting this offset is still lacking in mathematical analysis in the aspect of handover. Therefore, we describe and analyze the method called

* Corresponding Author

Adaptive Offset Handover Decision with the Link Quality Threshold (AOwLQT) in this paper as well as give a guideline to configure the offset. The rest of this paper is organized as follows. Section 2 described related works. Section 3 defines the system model. Mathematical analysis and numerical results are given in section 4 and 5 respectively. Section 6 concludes our study.

## 2 Related Works

When a user equipment (UE) moves within the overlap between base stations, a handover happens back and forth due to the randomly variation of received signal strength (RSS) from shadow fading and multipath fading in different locations. This phenomenon is called ping-pong effect. These unnecessary handovers of the UE will increase signaling load of the system and result in discontinuity of the session. In order to solve this problem, the RSS of target cell shall be stronger by a set value than the one of serving cell, and the UE can subsequently hand off to the target cell. The set value is called the hysteresis threshold to prevent the ping-pong effect. When the femto BS is installed in the center or inner region of the macrocell, the measured RSS of macro BSs is often greater than the measured RSS of femto BSs. A handover decision algorithm of a previous study [3] can solve the problem caused by asymmetric transmit power of femto BSs and macro BSs. The main idea of the algorithm is to compensate the RSS value of the target femto BSs with a portion of the RSS value of current serving macro BS before making handover decisions. When the RSS of femto BS satisfies a given threshold, the algorithm will consider whether the compensated value of the target femto BS is greater by the hysteresis margin than the RSS value of serving macro BS, to make UEs more easily handover to femto BS in the macrocell center mentioned above. This algorithm can reasonably increase the probability of assigning UEs to a femtocell by compensating the distance factor with the RSS value of the serving macro BS. However, the algorithm is not easily applied on the current 3GPP cellular system because the measurement report events in 3GPP specification [3GPP TS36.331] only supports basic comparison of RSS value instead of combination. In addition, the simulation result of [3] shows that the number of handovers is increased when the femto BS is closely located to the macro BS. A portion of the RSS value which is provided by current serving macro BS will occupy a large part of the compensated value of the target femto BSs when the femto BS is closely located to the macro BS. As the UEs go far away from the current serving macro BS, the portion of the RSS value which is provided by macro BS will decrease. This decrement of RSS value will not effectively help the UEs to overcome the hysteresis threshold quickly. The handover latency of the UEs thus increases, and it will cause system unstable and ping-pong effect. We analyze a handover decision algorithm with predefined offset adapting to the distance or path loss between femto base station and macro base station complying with the 3GPP specifications [2]. The handover decision algorithm will solve the problem that UEs near the center of macrocells may not easily camp on femtocells because of RSS value gap. The algorithm sets an expected coverage for femto BSs and derives a cell-specific offset of handover report events to raise the tendency of camping in a femto cell near the center of macro cell. Compared with [3], it doesn't combine the value of femto BS RSS with too large value of macro BS RSS when the femto BS is closely located to the macro BS. Therefore, the approach of this paper reduces the number of unnecessary handover.

## 3 System Model

As shown in Fig. 1, there are a marcocell, a femtocell and a UE in this system model. The distance between the marcocell and the femtocell is denoted by "*d*", and the distance *d* is divided into *k* sampling intervals. The UE moves from the marcocell to the femtocell in a straight line and measures the values of RSS from the femto BS and the marco BS in each sampling intervals, respectively. The algorithm makes handover decisions based on these measured values of RSS. Let $S_m[k]$ and $S_f[k]$ denote the values of RSS from the macro BS and the femto BS at time *k*, respectively. Note that the subscript m and f indicate the macro BS and the femto BS, respectively. With the values of transmit power $P_{m,tx}$, $P_{f,tx}$ and path loss $PL_m[k]$, $PL_f[k]$, the values of RSS from the macro BS and the femto BS can be expressed as follows:

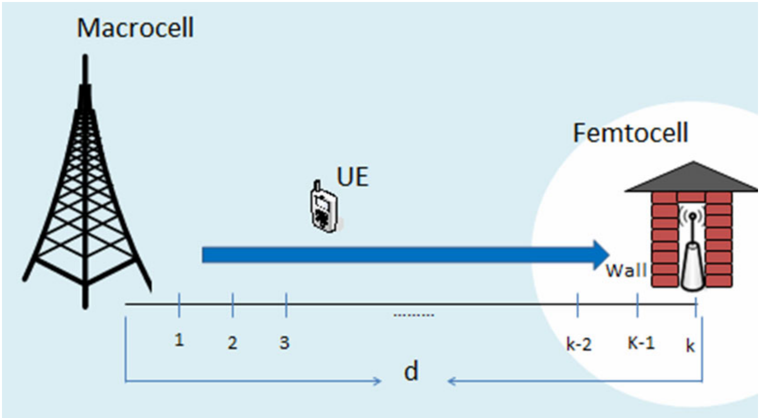


**Fig. 1.** System model

$$S_m[k] = P_{m,tx} - PL_m[k] - u_m[k] \tag{1}$$

$$S_f[k] = P_{f,tx} - PL_f[k] - u_f[k] \tag{2}$$

where $u_m[k]$ and $u_f[k]$ represent the log-normal shadowing with mean zero and variance $\sigma_m^2$ and $\sigma_f^2$, respectively. It is assumed that $u_m[k]$ and $u_f[k]$ are independent with each other and each of them has an exponential form of correlation function [4] with a correlation distance $d_0$. In order to avoid abrupt variation of the RSS, an exponential window function $W[k]$ is applied to $S_m[k]$ and $S_f[k]$, as studied in [5]. This operation can be expressed as follows:

$$\bar{S}_m[k] = W[k] * S_m[k] \tag{3}$$

$$\bar{S}_f[k] = W[k] * S_f[k] \tag{4}$$

$$W[k] = \frac{1}{d_1}\exp\left(\frac{-k \cdot d_s}{d_1}\right) \tag{5}$$

In equation (5), $d_s$ represents the distance between two adjacent measurement locations and $d_1$ represents a window length that decides the shape of the window. Appendix A shows the proof of window function's autocorrelation function. To compare the signal strengths from two base stations, a difference in the smoothed received signal levels can be expressed as follows:

$$S_r[k] = \bar{S}_m[k] - \bar{S}_f[k] \tag{6}$$

Measurement values of the above relative signal strength in two adjacent measurement locations are correlated whose correlation coefficient $\rho$ can be derived from the appendix B of [5] as follows.

$$\rho = \frac{1}{d_0 - d_1} \cdot \left\{ d_0 \exp\left(-\frac{|d_s|}{d_0}\right) - d_1 \exp\left(-\frac{|d_s|}{d_1}\right) \right\} \tag{7}$$

The variances of signal strengths from the macro and femto BSs after filtering through the window function are as follows.

$$\sigma_{mw}^2 = \frac{d_0 \sigma_m^2}{d_0 + d_1} \tag{8}$$

$$\sigma_{fw}^2 = \frac{d_0 \sigma_f^2}{d_0 + d_1}$$

(9)

In addition, the variance of relative signal strength is

$$\sigma_r^2 = \sigma_{mw}^2 + \sigma_{fw}^2 \tag{10}$$

## 4 Adaptive Offset with Link Quality Threshold (AOwLQT)

In a conventional handover decision algorithm, if the measured RSS of target cell exceeds that of the serving cell by a hysteresis threshold, the UE can subsequently hand off to the target cell. The Handover Decision is given by:

$$\bar{S}_f[k] > \bar{S}_m[k] + h \tag{11}$$

$h$ represents the hysteresis threshold. However, in the macrocell center mentioned above, the measured RSS of marco BSs is often greater than the measured RSS of femto BSs, resulting in that the handover criterion from a macrocell to a femtocell is hardly satisfied, even though the link quality of femtocell is fairly well. In order to improve the utilization of femto BSs, we propose a method called Adaptive Offset Handover Decision with the Link Quality Threshold (AOwLQT). We assume that the UE knows the distance between the femto BS and the macro BS and accordingly adapts the offset. In order to improve utilization of femto BSs, we set the basic services range of femtocell called femtocell boundary (FB). But the FB must be a reasonable value in the view points of users and the operator. Too large value of FB causes the UE easily handing over to a femtocell when the measured RSS of femto BS is small. It will cause radio link failure and ping-pong effect.

We compensate for the large asymmetry in transmit power of the macro BS and the femto BS when the UE enters FB, as shown in Fig. 2. Therefore, a method to determine the adaptive offset is suggested as follows:

$$\Delta = \begin{cases} \bar{S}_f[d-FB] - \bar{S}_m[d-FB] + p & \text{, UE handoff from Macrocell to Femtocell} \\ \bar{S}_m[d-FB] - \bar{S}_f[d-FB] + p & \text{, UE handoff from Femtocell to Macrocell} \end{cases} \tag{12}$$

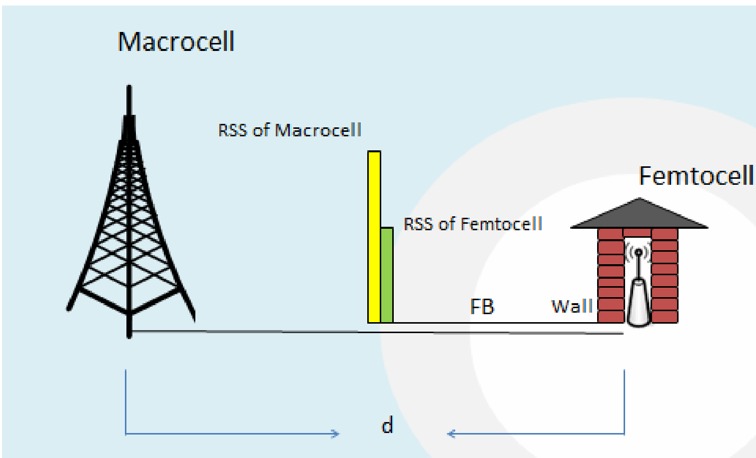


**Fig. 2.** System model with femtocell boundary

In equation (8), $\Delta$ denotes the adaptive offset, and $p$ indicates a basic value of the hysteresis threshold.

Fig. 3 and Fig. 4 illustrate the probability $P_f$ in which an UE will be assigned to the femto BS and the probability $P_m$ in which an UE will be assigned to the macro BS when the UE moves from the marcocell to the femtocell at different locations with the conventional handover decision and the adaptive offset (AO) handover decision, respectively. The distance between the marcocell and the femtocell is 200m.

The rising point of $P_f$ curve of AO is farther from the femto BS than that of conventional handover decision. It means that the Adaptive Offset (AO) Handover Decision might increase the number of unnecessary handover and extend handover unstable decision region due to weak signal of the target BS.

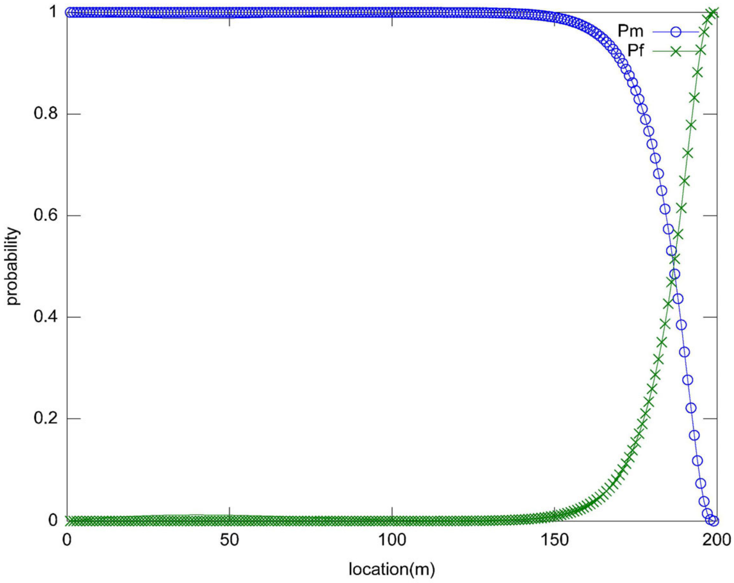


**Fig. 3.** Assignment probability to macro/femto BS vs. location of UE in conventional handover decision

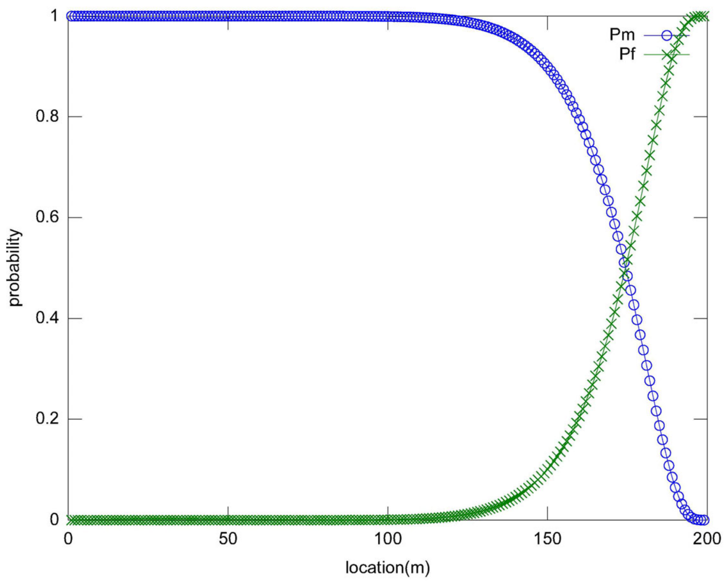


**Fig. 4.** Assignment probability to macro/femto BS vs. location of UE in adaptive offset handover decision

In order to solve this problem, we added a condition in Adaptive Offset (AO) Handover Decision: requiring that the RSS of femto BS must reach the Link Quality Threshold (LQT). Otherwise, we use conventional Handover Decision. Therefore, an Adaptive Offset (AO) Handover Decision with the Link Quality Threshold (LQT) is as follows:

*AOwLQT Handover Decision Algorithm*

If $\bar{S}_f[k] \geq LQT$ and $\bar{S}_f[k] > \bar{S}_m[k] + \Delta$

or if $\bar{S}_f[k] \leq LQT$ and $\bar{S}_f[k] > \bar{S}_m[k] + h$

then connect to Femto BS

If $\bar{S}_f[k] \geq LQT$ and $\bar{S}_m[k] > \bar{S}_f[k] + \Delta$

```
  or if S̄f[k]≤LQT and S̄m[k]>S̄f[k]+h
    then connect to Macro BS
```

Then, the Handover Decision algorithm which combines the conventional Handover Decision method with AOwLQT handover decision algorithm is as follows:

```
Handover Decision Algorithm
  If (Target Cell is Femtocell and Serving Cell is Femtocell)
    Use Conventional Handover Decision Algorithm;
  else if (Target Cell is Macrocell and Serving Cell is Macrocell)
    Use Conventional Handover Decision Algorithm;
  else
    Use AOwLQT Handover Decision Algorithm;
```

Following the procedure used in [5] to analyze AOwLQT, let $P_{ho}[k]$ denote the probability that there is a handover at interval *k*. $P_{f|m}[k]$ denotes the probability of handover from the macrocell to the femtocell, and vice versa for $P_{m|f}[k]$. Then, assuming $P_m[k]$ and $P_f[k]$ denote the probability that the UE is assigned to the macrocell or the femtocell at interval *k*, the following recursive relations hold:

$$P_m[k] = P_m[k-1]\cdot\left(1-P_{f|m}[k]\right)+P_f[k-1]\cdot P_{m|f}[k] \tag{13}$$

$$P_f[k] = P_m[k-1]\cdot P_{f|m}[k]+P_f[k-1]\cdot\left(1-P_{m|f}[k]\right) \tag{14}$$

$$P_{ho}[k] = P_m[k-1]\cdot P_{f|m}[k]+P_f[k-1]\cdot P_{m|f}[k] \tag{15}$$

with $P_m[1]=1$ and $P_f[1]=0$ as initial values. It is clear that once we find a way to compute $P_{f|m}[k]$ and $P_{m|f}[k]$, the problem is solved. Then, $P_{f|m}[k]$ and $P_{m|f}[k]$can be calculated by using the concept of conditional probability, as follows:

$$P_{f|m}[k] = \frac{P\{S_r[k] < -\Delta, S_r[k-1] \geq -\Delta\}}{P\{S_r[k-1] \geq -\Delta\}} \tag{16}$$

$$P_{m|f}[k] = \frac{P\{S_r[k] > \Delta, S_r[k-1] \leq \Delta\}}{P\{S_r[k-1] \leq \Delta\}} \tag{17}$$

$$P\{S_r[k-1] \geq -\Delta\} = \int_{-\Delta}^{\infty} f\left(S_{r,k-1}\right) dS_{r,k-1} \tag{18}$$

$$P\{S_r[k-1] \leq \Delta\} = \int_{-\infty}^{\Delta} f\left(S_{r,k-1}\right) dS_{r,k-1} \tag{19}$$

$P\{S_r[k-1] \geq -\Delta\}$ and $P\{S_r[k-1] \leq \Delta\}$ denote the probability that the mobile is assigned to the macrocell or the femtocell at interval *k*-1. Because the distribution of $S_r[k-1]$ is normal, the Probability Density Function $f\left(S_{r,k-1}\right)$ can be expressed with mean $m_{k-1}$ and variance $\sigma_{k-1}^2$, as follows:

$$f\left(S_{r,k-1}\right) = \frac{1}{\sqrt{2\pi\sigma_{k-1}^2}}\exp\left(-\frac{\left(S_{r,k-1}-m_{k-1}\right)^2}{2\sigma_{k-1}^2}\right) \tag{20}$$

Therefore, $P\left\{S_r\left[k\right]<-\Delta, S_r\left[k-1\right]\geq-\Delta\right\}$ and $P\left\{S_r\left[k\right]>\Delta, S_r\left[k-1\right]\leq\Delta\right\}$ is given by

$$P\left\{S_r\left[k\right]<-\Delta, S_r\left[k-1\right]\geq-\Delta\right\}=\int_{-\infty}^{-\Delta}\int_{-\Delta}^{\infty} f\left(S_{r,k-1}, S_{r,k}\right) dS_{r,k-1} dS_{r,k} \quad \textbf{(21)}$$

$$P\left\{S_r\left[k\right]>\Delta, S_r\left[k-1\right]\leq\Delta\right\}=\int_{\Delta}^{\infty}\int_{-\infty}^{\Delta} f(S_{r,k-1}, S_{r,k}) dS_{r,k-1} dS_{r,k} \quad \textbf{(22)}$$

The distributions of $S_r\left[k-1\right]$ and $S_r\left[k\right]$ are normal, respectively. Then, $S_r\left[k-1\right]$ is a normal distribution with mean $m_{k-1}$ and variance $\sigma_{k-1}^2$, and $S_r\left[k\right]$ is a normal distribution with mean $m_k$ and variance $\sigma_k^2$. The Joint Probability Density Function of $S_r\left[k-1\right]$ and $S_r\left[k\right]$ can be expressed by (19).

$$\begin{aligned} f(S_{r,k-1}, S_{r,k}) &= \frac{1}{2\pi\sigma_{k-1}\sigma_k\sqrt{1-\rho^2}} \\ &\cdot\exp\left\{-\frac{1}{2\left(1-\rho^2\right)}\cdot\left\{\begin{aligned}&\left(\frac{S_{r,k-1}-m_{k-1}}{\sigma_{k-1}}\right)^2-2\rho\left(\frac{S_{r,k-1}-m_{k-1}}{\sigma_{k-1}}\right)\cdot\left(\frac{S_{r,k}-m_k}{\sigma_k}\right)\\&+\left(\frac{S_{r,k}-m_k}{\sigma_k}\right)^2\end{aligned}\right\}\right\}\end{aligned} \quad \textbf{(23)}$$

On the above basis, the results of numeral analysis will be presented in the next section.

## 5 Numerical Analysis

In this section, numerical results are investigated by using the system model and analysis method presented in the section 4. The parameters are listed in Table 1. The values of $P_{m,tx}$ and $P_{f,tx}$ are set to 43 dBm and 21.5 dBm, respectively. The standard deviations of shadowing fading are set to 8dB and 6dB for macrocell and femtocell, and the correlation distance $d_0$ is 20m. The received signals are smoothed using an window function with sample duration $d_S = 1m$ and window length $d_1 = 30m$. The correlation distance $d_0$ and window length $d_1$ can be used to calculation the variance of smoothed received signal and the value of correlation coefficient by autocorrelation functions [5]. The femtocell boundary and the link quality threshold are set to 25 m and -72 dBm, respectively.

**Table 1.** Parameters for performance analysis

| | |
|---|---|
| $P_{m,tx} = 43dBm$ | Tx power of macrocell |
| $P_{f,tx} = 21.5dBm$ | Tx power of femtocell |
| $PL_m = 28 + 35\log_{10}\left(d\right)$ | Path loss model for macrocell |
| $PL_f = 38.5 + 20\log_{10}\left(d\right)$ | Path loss model for femtocell |
| $\sigma_m = 8dB$ | Shadowing for macrocell |
| $\sigma_f = 6dB$ | Shadowing for femtocell |
| $Lwalls = 25dB$ | Wall loss applied to path loss model |
| $d_0 = 20m$ | Correlation distance |
| $d_1 = 30m$ | Window length |
| $d_s = 1m$ | Sample duration |
| $FB = 25m$ | Femtocell boundary |
| $LQT = -72dBm$ | Link Quality Threshold |

Fig. 5 represents the probability that the UE will be assigned to the femto BS, which is installed 200m away from the macro BS when the UE moving straightly from a macro BS to a femto BS. In this situation, the handover criterion of a conventional algorithm is hardly triggered because the RSS from the macro BS is still strong. In comparison with conventional algorithm, the adaptive offset method can increase utilization of femto BS. For example, the probability of assignment to the femto BS is below 0.3 when the UE moves to the location 180m and decides its serving base station by the conventional algorithm. If the AO is used in the same case, the probability becomes to 0.6. However, as described in section 4, the probability of the AO grows slowly, hence increasing the number of unnecessary handover. The AOwLQT can solve this problem. As shown in Fig. 5, when the AOwLQT works, its conventional algorithm part is used until the RSS of femto BS meets the LQT at the location 169m. After the location 169m, the AO part is used and the probability rises quickly. Fig. 6 shows the expected number of handovers as a function of distance between the macro BS and the femto BS, in the case that a UE moves from the macro BS to the femto BS. The expected number of handovers can be expressed as follows:

$$N_{ho} = \sum_k P_{ho}[k] \tag{24}$$

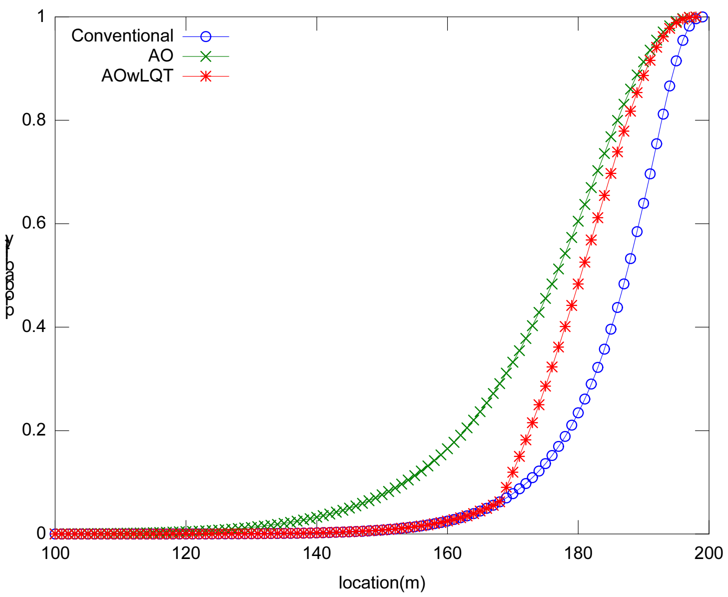


**Fig. 5.** Assignment probability to femto BS vs. location of UE

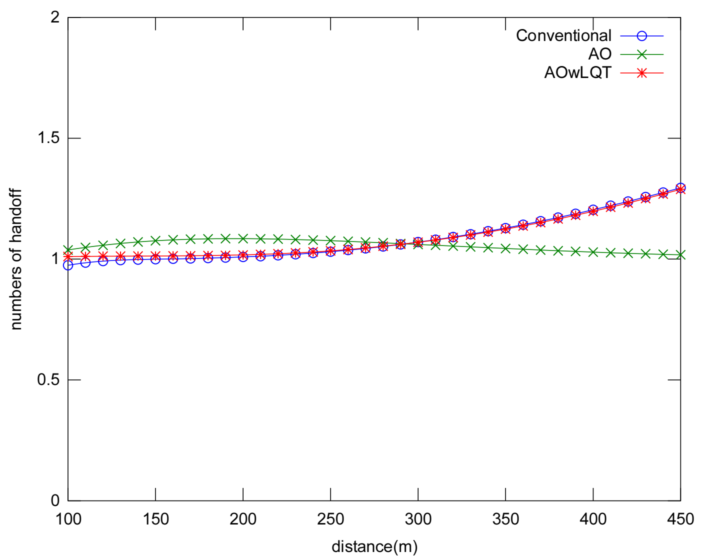


**Fig. 6.** Number of handovers vs. distance of macro-femto BS

When the distance is smaller than 290m and the femto BS is closely located to the macro BS, the expected number of handovers can be reduced by AOwLQT as compared to the AO. The AOwLQT also increases the utilization of femto BS, compared to the conventional algorithm from observing the assignment probability shown in Fig. 5. However, when the distance is larger than 300m in Fig. 6, the AO performs better than others in the handover stability. This is because the assignment probability of the AOwLQT and the conventional algorithm in those above 300m cases grows slower than the AO does as well as the handover area is wider than that of the AO, resulting in unnecessary handovers.

In addition, we study what the probability of the UE staying in the femto BS will be in the case that the UE moves vertically in different paths between the macro BS and the femto BS. Here we assess four cases of paths and assume that the distance between the macro BS and femto BS is 200 meters as shown in Fig. 7: The UE moves from the south to the north following a 100-meter-long vertical line, which is bisected by the line segment from the macro base station to the femto base station at four locations 160, 170, 180, and 190 meters away from the macro base station. Fig. 8 indicates a vertical movement located at 160m. The UE moving length is 100 meters long, which is divided into $K$ sampling intervals. The UE measures the RSS from the femto BS and the marco BS in each sampling intervals. The numerical results are also investigated by the analysis method in the section 4. Then, the values of $P_m[k]$ and $P_f[k]$ are recalculated by using equation (9) and (10), respectively.

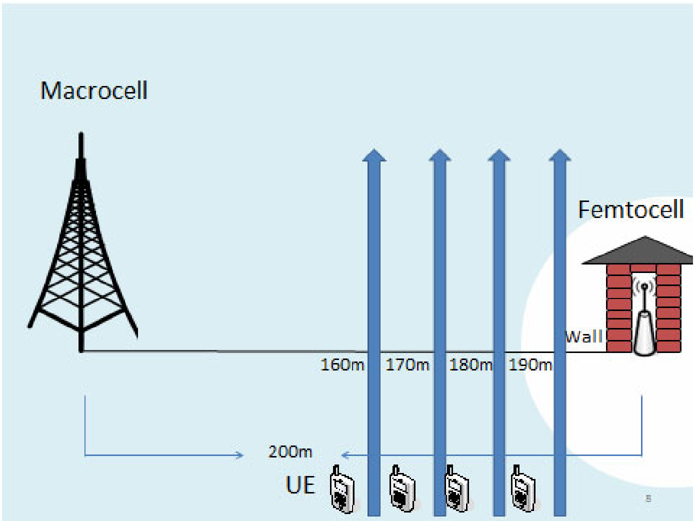


**Fig. 7.** Four cases of vertical movement

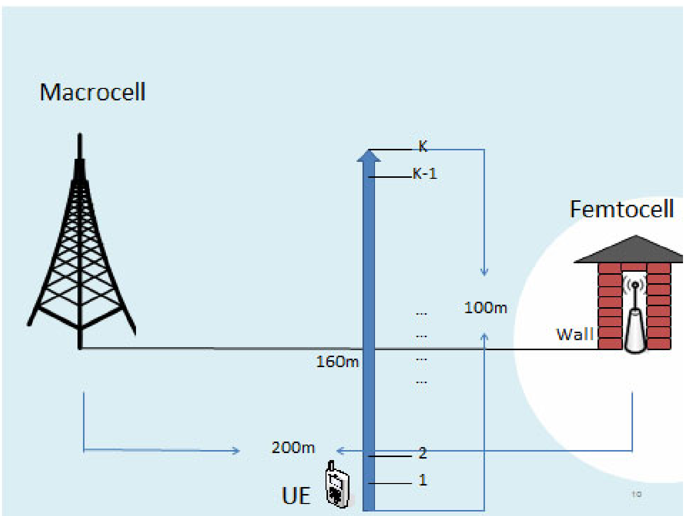


**Fig. 8.** Vertical movement at 160m

Fig. 9, 10, 11, and 12 indicate the probability that the UE is assigned to the femto BS under vertical movement of the UE. The horizontal axis is the location of UE at the vertical path, ranging from 0m to 100m, and the vertical axis is the probability of the UE camping in the femto BS. Fig. 9 shows the UE vertical movement at 160m. The probabilities of camping in the femto BS in three methods are all low because the RSS value of the femto BS is much lower than that of the macro BS. The AO method has higher probability than the other two methods, but the low RSS may bring instability of camping in the femto cell. On the other hand, the curves of AOwLQT and the conventional decision are the same because the RSS of femto BS does not meet the quality threshold all the time, downgrading AOwLQT to the conventional.

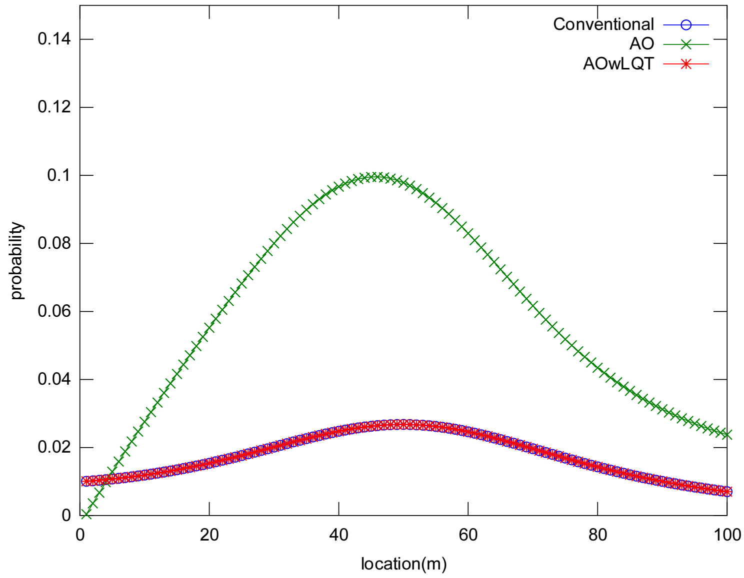


**Fig. 9.** Assignment probability to femto BS vs. UE location in the case at 160m

Fig. 10 shows that in the case at 170m the RSS of the femto BS satisfies the LQT at location 39m of the vertical line, and the probability of the AOwLQT rises more quickly than the conventional algorithm does. However, the RSS of femto BS is still low all the time in this movement, and AO method might result in radio link failure for its higher femto BS assignment probability than the others.

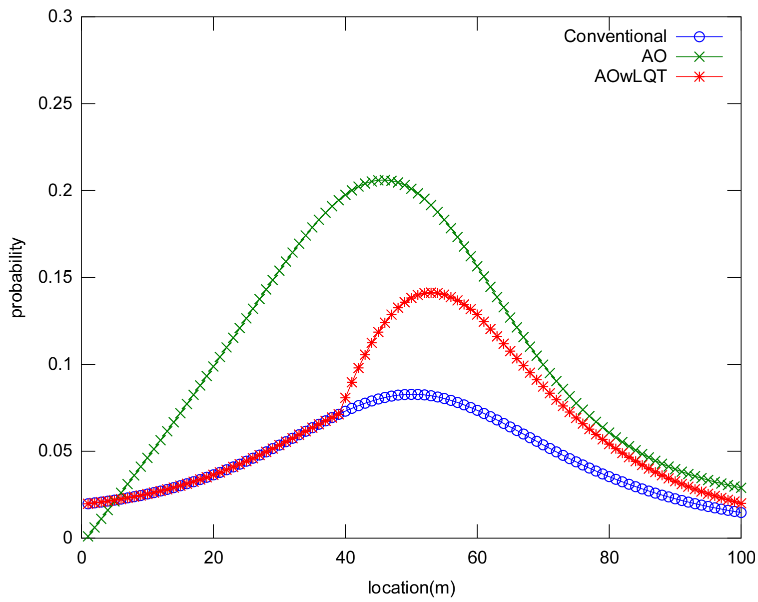


**Fig. 10.** Assignment probability to femto BS vs. UE location in the case at 170m

Fig. 11 indicates that the AOwLQT curve begin steep rising as LQT condition of the femto cell is fulfilled, even exceeding the curve of the conventional algorithm, which achieves an utilization improvement of femto BS comparing to the conventional. Besides, comparing to AO, in the low RSS area of the femto BS, the probability of AOwLQT method is lower than that of AO method, reducing probable radio link failures. In the central region of the femtocell with well RSS, the assignment probability of AOwLQT method even slightly exceeds AO method's.

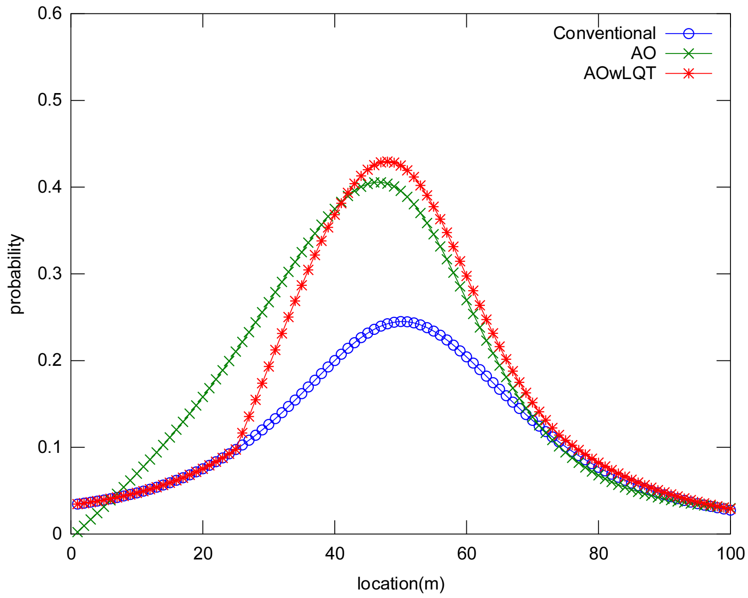


**Fig. 11.** Assignment probability to femto BS vs. UE location in the case at 180m

Fig. 12 obviously shows that the AOwLQT curve has the highest assignment probability near the central region of the femtocell. The AO curve is higher than the others before reaching the point of LQT satisfaction, which means that the AO decision might more easily encounter radio link failure than others before the point. AO compensates the RSS difference between femto BS and macro BS for easy handover into the femto cell when coming in, but also for easy handover out when going out of the femto cell. AOwLQT tends to keep those UEs with qualified RSS in the femto cell.

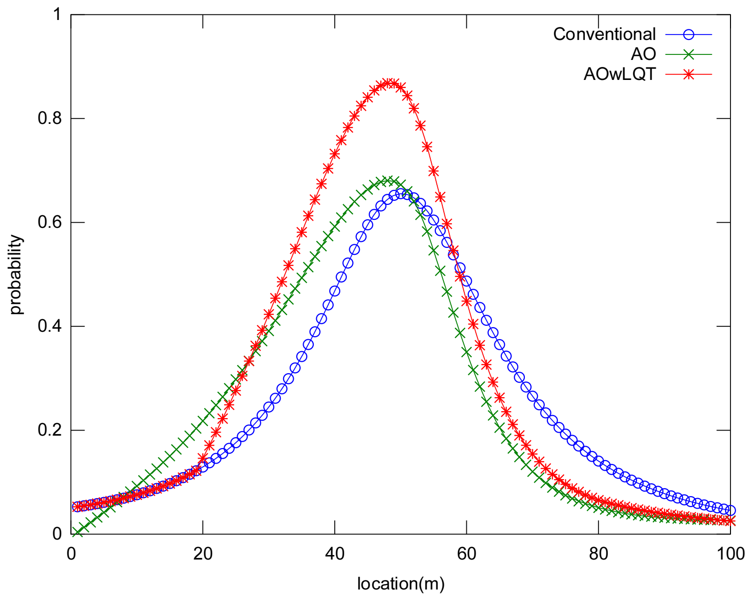


**Fig. 12.** Assignment probability to femto BS vs. UE location in the case at 190m

Fig. 13 shows the expected number of handovers when the UE moves vertically in different perpendicular lines. These different perpendicular lines locates at different distance away from the macro BS. The abscissa represents the distance of the midpoint away from the marco BS and the ordinate is the expected number of handovers in the vertical movement. When the RSS of the femto BS in the UE movement satisfies the LQT, the expected handover number of the AOwLQT is larger than the conventional algorithm's. However, when the location is near the femtocell boundary (e.g. 170m, 175m and 180m), the expected number of the AOwLQT is less than the AO's. When the location is near the femto BS, the number of AOwLQT is the highest. The reason is that the $P_f[k]$ of AOwLQT is the highest when the UE is near the femto BS.

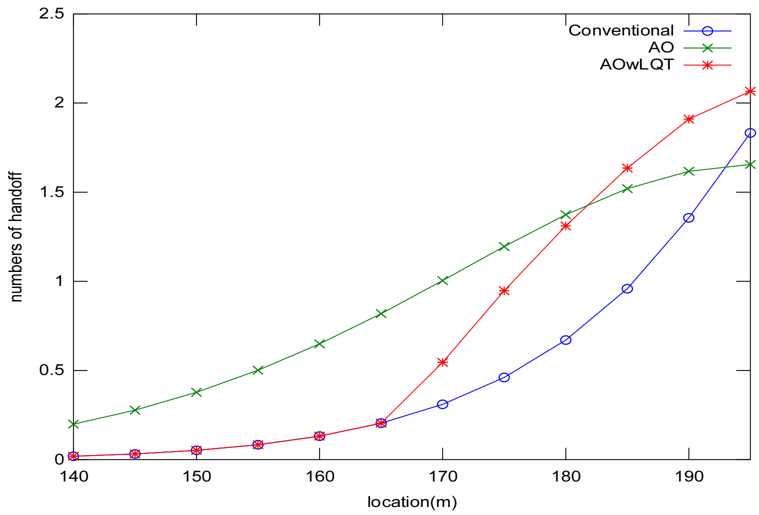


**Fig. 13.** Number of handovers vs. location of perpendicular line

## 6 Conclusions

Hierarchical macro/femto-cell networks are considered as a promising technology for the improvement of indoor coverage and network capacity. In these emerging networks, handover procedures for a mobile station moving from a macrocell to a femtocell should maximize the utilization of femto BSs. In this paper, we analyze handover decision algorithms with adaptive offset. When the RSS of femtocells satisfies the link quality threshold, the algorithm compensates large differences between RSS measurements of macrocells and femtocells by a priori setting a femtocell boundary, indicating that user equipments stay inside the expected coverage of femtocells. The handover decision algorithm increases the utilization of femto BS. In addition, it reduces the expected number compared with pure AO when the femto BS near the macro BS.

## Acknowledgement

The authors would like to thank the anonymous reviewers of the paper for their very helpful and constructive criticism. Their suggestions have enabled them to improve the quality of this work. This study was partially published in the proceedings of 2014 International Conference on Communications and Robotics Engineering (CARE), and supported in part by the Ministry of Science and Technology, Taiwan, R.O.C., under grant 105-2622-E-194-001-CC1.

## References

[1] V. Chandrasekhar, J.G. Andrews, A. Gatherer, Femtocell networks: a survey, IEEE Communications Magazine 46(9)(2008) 59-67.

[2] 3GPP TS 36.300 V8.7.0, Evolved Universal Terrestrial Radio Access (E-UTRA) and Evolved Universal Terrestrial Radio Access Network (EUTRAN); Overall Description; Stage 2, December 2008.

[3] J.M. Moon, D.H. Cho, Novel handover decision algorithm in hierarchical Macro/Femto-cell networks, in: Proc. IEEE Wireless Communication and Networking Conf. (WCNC 2010), 2010.

[4] M. Gudmundson, Correlation model for shadow fading in mobile radio systems, Electronics Letters 27(23)(1991) 2145-2146.

[5] K. Itoh, S. Watanabe, J.-S. Shih, T. Satc, Performance of Handoff Algorithm Based on Distance and RSSI Measurements, IEEE Transactions on Vehicular Technology 51(6)(2002) 1460-1468.

[6] 3GPP TS 25.304 V12.1.0, 3rd Generation Partnership Project; Technical Specification Group Radio Access Network; User Equipment (UE) procedures in idle mode and procedures for cell reselection in connected mode, March 2014.

[7] 3GPP-TSG RAN R2-122726, HetNet Mobility Performance with Cell Range Expansion and ABS, May 2012.

# Appendix: The Proof of Window Function's Autocorrelation Function

The proof of window function's autocorrelation function is given by

$$
\begin{aligned}
\rho(k) &= \int_0^{\infty} W(x)\cdot W(x+k)\,dx \\
&= \int_0^{\infty} \frac{1}{d_1}\cdot \exp\left(-\frac{x}{d_1}\right)\cdot \frac{1}{d_1}\cdot \exp\left(-\frac{x+k}{d_1}\right)dx \\
&= \frac{\exp\left(\frac{-k}{d_1}\right)}{d_1^2}\int_0^{\infty} \exp\left(\frac{-2x}{d_1}\right)dx \\
&= \frac{\exp\left(\frac{-k}{d_1}\right)}{d_1^2}\left[\frac{\exp\left(\frac{-2x}{d_1}\right)}{\frac{-2}{d_1}}\right]_0^{\infty} \\
&= \frac{\exp\left(\frac{-k}{d_1}\right)}{d_1^2}\left[0-\left(\frac{-d_1}{2}\right)\right] \\
&= \frac{\exp\left(\frac{-k}{d_1}\right)}{d_1^2}\cdot\frac{d_1}{2} = \frac{\exp\left(\frac{-k}{d_1}\right)}{2d_1}
\end{aligned}
\qquad \textbf{(25)}
$$